Effector function does not contribute to protection from virus challenge by a highly potent HIV broadly neutralizing antibody in nonhuman primates.

Authors

Lars Hangartner[1, 9], David Beauparlant[1], Eva Rakasz[2], Rebecca Nedellec[1], Nathanaël Hozé[3], Katherine McKenney[1], Mauricio A. Martins[4], Gemma E. Seabright[5,6], Joel D. Allen[5], Andrea M. Weiler[2], Thomas C. Friedrich[2], Roland R. Regoes[7], Max Crispin[5], Dennis R. Burton[1, 8, 9, 10]

Affiliations

1. Department of Immunology and Microbiology, The Scripps Research Institute, 10550 North Torrey Pines Road, La Jolla, CA 92037, U.S.A.
2. Wisconsin National Primate Research Center, University of Wisconsin-Madison, 1220 Capitol Court, Madison, WI 53715, U.S.A.
3. ETH Zurich, Institute of Integrative Biology (IBZ), Theoretical Biology, ETH Zurich, ETH Zentrum, CHN H76.2, Universitätstrasse 16, 8092 Zurich, Switzerland. Present address: Mathematical Modelling of Infectious Diseases Unit, Institut Pasteur, UMR2000, CNRS, 75015 Paris, France.
4. Department of Immunology and Microbiology, Scripps Research, Jupiter, FL 33458, U.S.A.
5. University of Southampton, School of Biological Sciences, University of Southampton, Southampton, SO17 1BJ, United Kingdom
6. Department of Biochemistry, University of Oxford, Oxford OX1 3QU, United Kingdom
7. ETH Zurich, Institute for Integrative Biology (IBZ), Theoretical Biology, ETH Zurich, ETH Zentrum, CHN K12.2, Universitätstrasse 16, 8092 Zurich, Switzerland.
8. IAVI Neutralizing Antibody Center, The Scripps Research Institute, La Jolla, CA 92037, U.S.A.
9. Consortium for HIV/AIDS Vaccine Development (CHAVD), The Scripps Research Institute, La Jolla, CA 92037, USA.
10. Ragon Institute of Massachusetts General Hospital, Massachusetts Institute of Technology, and Harvard University, Cambridge, MA 02139, U.S.A.

\+ Corresponding authors: lhangart@scripps.edu or burton@scripps.edu

Abstract
Protection from immunodeficiency virus challenge in nonhuman primates (NHPs) by a first-generation HIV broadly neutralizing antibody (bnAb) b12 has previously been shown to benefit from interaction between the bnAb and Fcγ receptors (FcγR) on immune cells. To investigate the mechanism of protection for a more potent second-generation bnAb currently in clinical trials, PGT121, we carried out a series of NHP studies. These studies included treating with PGT121 at a concentration at which only half of the animals were protected in order to avoid potential masking of FcγR effector function benefits by dominant neutralization and using a new variant that more completely eliminated all rhesus FcγR binding than earlier variants. In contrast to b12, which required FcγR binding for optimal protection, we concluded that PGT121-mediated protection is not augmented by FcγR interaction. Thus, for HIV passive antibody prophylaxis, these results, together with existing literature, emphasize the importance of neutralization potency for clinical antibodies, with effector function requiring evaluation for individual antibodies.

One Sentence Summary
Effector function is not required for a potent HIV envelope-specific broadly neutralizing antibody to protect nonhuman primates from mucosal SHIV infection.

Introduction

Evidence from nonhuman primate (NHP) models of human immunodeficiency virus (HIV) infection indicate that both virus neutralization and Fc-dependent effector functions can contribute to neutralizing Ab (nAb) protection against virus challenge *(1, 2)*. These Fc-dependent effector functions include antibody-dependent cellular cytotoxicity (ADCC), antibody-dependent cellular phagocytosis (ADCP), and activation of the complement system (C'). Protection against high-dose vaginal simian-human immunodeficiency virus (SHIV) in the NHP model by the first-generation HIV broadly neutralizing antibody (bnAb) b12 was most effective if neutralization was augmented by Fcγ receptor (FcγR) functions, as shown by reduced protection in NHPs treated with effector function-crippled variants of b12 *(1)*. A b12 variant lacking complement -activation (KA variant) was as protective as the wild-type antibody, suggesting complement is not involved in b12-mediated protection. In animals treated prophylactically, treatment with wild-type or KA-variant b12 resulted in lower and delayed primary viremia compared to controls. However, a $L_{234}A/L_{235}A$ (LALA) variant of b12, which lacks both complement and FcγR binding, was less protective, leading to more infected animals and higher primary viremia compared to wild-type and KA-breakthrough animals. These results implied that FcγR function contributed to protection. Of note, approximately half the animals in the study were protected by the LALA antibody, which implied that neutralization alone can be sufficient for protection mediated by b12. Further, low-dose repeated vaginal challenge in b12-treated NHPs yielded a comparable result to high-dose SHIV challenge *(2)*.

Further NHP studies using FcγRIIIa-binding-enhanced antibodies did not show an advantage relative to wild-type antibodies, suggesting that improved FcγRIIIa binding, often associated with enhanced ADCC, does not necessarily lead to improved protection *(3)*. In humanized mice, FcγR-mediated functions, under certain conditions, increased anti-viral activities of bnAbs *(4)*. Interestingly, the authors showed that no FcγR benefits are apparent at high bnAb concentration, suggesting that FcγR contribution might be of particular importance specifically when virus neutralization by bnAbs is not overwhelming. Of note, the humanized mice studies involve infection of cells before antibody is introduced and so are not strictly investigating prophylaxis. Very recently, two studies assessed the ability of variant bnAbs to impact established infection in NHPs. Modest effects of eliminating antibody effector function on viral clearance were observed, and enhanced FcγR binding led to decreased, rather than increased, viral clearance *(5, 6)*.

PGT121 *(7)* is a second-generation highly potent bnAb, that is currently being evaluated for HIV prophylaxis clinical trials *(8)*. PGT121 was also recently evaluated in the SHIV macaque model *(7)*. In contrast to b12-LALA, PGT121-LALA afforded sterilizing immunity against cell-associated intravenous $SHIV_{SF162P3}$ challenge, which was similar to wild-type PGT121, suggesting antibody effector functions may be redundant for PGT121-mediated protection *(9)*. A number of differences exist between the conditions used for the published b12 and PGT121 studies, including (1) the former studies used free virus and mucosal challenge whereas the latter used cell-associated virus and intravenous challenge (2) PGT121 protection was measured at high bnAb titers *(10)*, that from mouse studies *(4)* might mask benefits of bnAb interaction with FcγR

(4). Finally, It has previously been found that LALA variants retain considerable binding to human FcγRI *(11)* that may have influenced the results observed should the finding hold for macaque FcRI.

Here, we carried out protection studies with PGT121 and its LALA variant at high bnAb dose as in Parsons *et al. (9)* and then at moderate bnAb concentration that may provide deeper insight into any FcγR requirements for protection, as suggested by murine studies *(4)*. We also performed a protection study using a PGT121-LALAPG variant that yielded more complete abrogation of all FcγR binding activity.

Results

Effector functions do not contribute to PGT121 protection even at sub-protective doses.

To determine the effects of reduced effector function on the protective activity of the potent second-generation bnAb, PGT121, a passive immunization experiment was conducted by infusion of 1 mg/kg of each of the Abs PGT121, PGT121-LALA, or anti-Dengue control (DEN3) into antibiotic-treated, menstrual cycle-synchronized female Indian rhesus macaques. In comparison to b12 administered at 25 mg/kg, PGT121 was given at a dose of 1 mg/kg *(9, 10)* to account for its lower neutralization IC_{50} (0.04 vs 0.005 μg/ml respectively). Following single high-dose vaginal challenge with $SHIV_{SF162P3}$ (300 tissue culture infectious doses 50 [$TCID_{50}$]), animals receiving the DEN3 control antibody readily became infected while groups of 5 animals given either PGT121 or PGT121-LALA were fully protected (Fig. 1).

To investigate whether neutralization at 1mg/kg of PGT121 masked possible protection mediated by Fc effector function (fig. S1), a sub-protective dose of antibody (0.2 mg/kg) was administered in a second set of passive immunization experiments (IS-35, 49, 82, Fig. 2), as differences in protection between Fc-competent and Fc-crippled versions of PGT121 may be more prominent at this semi-protective concentration *(10)*. However, again, there was no significant difference in protection conferred by Fc-competent and Fc-crippled PGT121 ($p=0.15$, Fig. 2); 7 out of 15 PGT121 and 11 out of 15 PGT121-LALA-immunized animals were protected, suggesting that the lack of Fc-effector function benefits in the previous experiment was not due to the high dose of the antibody.

Wild-type and KA variant b12 antibodies not only reduced the number of infections compared to an isotype control antibody, but also lowered primary viremia and delayed breakthrough in animals *(1)*. For b12-LALA, primary viremia, summarized by the area under the curve (AUC), followed that of control animals more closely, while the AUCs of b12-KA and b12 breakthrough animals were more similar to each other. In this study, we detected no significant difference between PGT121 and PGT121-LALA in terms of primary viremia.

Unexpectedly, day 0 serum concentrations of PGT121 were 25-30% lower than PGT121 LALA (fig. S2) despite identical doses of antibodies being infused in both groups. This difference may be caused by altered serum or tissue distributions of both antibodies. If the serum half-life was calculated including day 0, the apparent serum half-life differed between PGT121 (1.6 days) and PGT121-LALA (2.1 days, fig. S2). However, excluding day 0, both serum half-lives were comparable at 2.9 and 2.5 days for PGT121 and PGT121-LALA, respectively. This suggested the LALA variant diffused into tissue slower than wild-type antibody, yet offered comparable or better protection.

Similar to previous experiments performed with the bnAb 10-1074 *(12)*, another V3-glycan specific antibody, a potential effect arising from PGT121 administration was observed in that 5 animals receiving either PGT121 or PGT121-LALA spontaneously controlled viremia after 90 days, while we did not observe spontaneous control in DEN3 animals. Of note, Chinese/Indian hybrid animals (rh2540, rh2541, rh2544), purchased as Indian rhesus macaques but identified as hybrids during major histocompatibility complex (MHC) and FcγR genotyping, also spontaneously controlled infection after 45 days, even after receiving DEN3.

To determine whether protection across the studies was considered sterile, and to determine the mechanism of the spontaneous control, two controller animals (r04124 and r07036), three protected PGT121-LALA animals (r07038, rhBD70, rhBE72), and two protected PGT121 recipient animals (rhBC67 and rhBE61) were depleted of $CD8^+$ lymphocytes via antibody administration 482 days post infection. No viremia was detected in protected animals. Also, no signs of T cell priming were found in protected animals by tetramer or intracellular cytokine staining of peripheral blood mononuclear cells (PBMCs) from IS-35. In contrast, T cell priming was found in all infected animals evaluated (table S1). Spontaneous controller PGT121-treated animals, r04124 and r07036, became viremic within 3 days following $CD8^+$ lymphocyte depletion (fig. S3). Animal r04124 spontaneously lost viral control around the time of CD8+ lymphocyte depletion yet displayed exacerbated viremia as a result of the depletion. Although this experiment only employed a very limited number of animals, it provides evidence that virus persisted in both animals for over 200 days and indicates that the virus may have been held in check by $CD8^+$ effector cells.

More complete ablation of rhesus FcγR-binding does not affect protection afforded by PGT121.

It was reported that LALA variant IgGs can retain binding to human FcγRI *(11)*. In order to investigate PGT121-LALA binding to rhesus FcγRs, the respective soluble proteins were recombinantly expressed and antibody binding monitored by ELISA (Fig. 3A). PGT121-LALA retained considerable binding to rhesus FcγRI, and weak binding to rhesus FcγRIIa. The latter was sufficient to trigger uptake of opsonized beads by THP-1 cells but was not sufficient to mediate ADCC (Fig. 3B-D). A variant of PGT121 containing a $P_{329}G$ substitution in addition to the $L_{234}A/L_{235}A$ modification was prepared (LALAPG) and was found to abolish all binding to macaque FcγRs, including FcγRI and II (Fig. 3A), and abolished residual bead-phagocytosis (Fig.

3B). This variant retained all other properties of the antibody, including its serum half-life *(11, 13)*.

Protection afforded by PGT121-LALAPG was then assessed in 15 animals receiving 0.2mg/kg PGT121-LALAPG, 3 animals receiving PGT121, and 5 animals receiving control DEN3 (Fig. 3C). The LALAPG-variant was found at similar serum titers at the day of infection and had a serum half-life of 2.3 days, similar to PGT121. Further, PGT121-LALAPG protected 12 out of 15 animals from a single high-dose vaginal $SHIV_{SF162P3}$ infection (Fig. 4A). Comparing these data with the data above, the results suggest that the LALAPG variant performs comparably to wild-type PGT121 and that effector function is not contributing to antibody protection.

A meta-analysis across all individual experiments based on day 0 antibody concentration and neutralizing data binned by outcome revealed that protected animals had significantly higher PGT121 variant concentrations (using Welch two sample t-tests, p=0.000603) or neutralizing titers (p= 0.0008) compared to infected animals (fig. S2D). However, differences in day 0 neutralizing titers were not different for all individual experiments (fig. S2C). When viremia in the breakthrough animals was analyzed, it was found that PGT121-treated animals had significantly lower viremia (p=0.021, Fig. 4B) compared to DEN3-treated animals. In contrast, viremia in PGT121-LALA treated animals was not significantly different as compared to DEN3-treated animals (p=0.15, Fig. 4B). Similarly, PGT121-LALAPG-treated animals did not significantly differ in AUC compared to DEN3-treated control animals (p=0.2), and viremia in these animals was also not different from PGT121 (p=0.08) or PGT121-LALA (p=0.24)-treated animals in Welch two sample t-tests (Fig. 4B). However, it should be noted that the number of break-through animals reported here is small, thus limiting the power of these analyses.

Differences in effector function activities of PGT121 and b12 fail to provide an explanation for their differing in vivo behavior.

To explore potential reasons for the observed differences between b12 and PGT121 in terms of the contribution of effector function towards protection, we investigated effector activities of the two bnAbs. We recognized that it would be difficult to reproduce the conditions in terms of effector and target cells present in the exposed animals, but we considered it worthwhile to investigate a number of assays in vitro. One key factor that we took into account in this study was that typical serum concentrations used in b12 experiments at challenge (310-1029 μg/ml) were much higher than those used for PGT121 (5-17.6 μg/ml).

We therefore investigated the ability of the human NK cell line KHYG-1 expressing rhesus CD16 *(14)* to kill $SHIV_{SF162P3}$-infected CEM.NK^R $CCR5^+Luc^+$.1c12 target cells, a subclone of the widely used CEM.NK^R $CCR5^+Luc^+$ target cell line *(14)*. As shown in Fig. 3C, PGT121 was somewhat more effective than b12. However, making allowance for the differing antibody concentrations present in vivo, the two bnAbs might have been predicted to be approximately equally effective in our experiments. The LALAPG antibodies were ineffective at promoting ADCC. Therefore, this

ADCC assay did not correlate with the differences in protection described between b12 and PGT121 in NHP studies.

We also performed ADCC assays using $SHIV_{SF162P3}$-infected CEM.NK^R $CCR5^+Luc^+$.1c12 target cells with human primary NK effector cells. b12 and PGT121 displayed comparable NK cell-mediated ADCC activities at typical assay concentrations (<35μg/ml, Fig. 3C). At high antibody concentrations present in b12 animals at the day of infection (>300μg/ml), there was an in vitro prozone effect observable for all antibodies tested (fig. S4A). Overall, the results from assays using human primary NK cells were similar to those for the rhesus CD16 human KHYG-rhCD16 NK cell line.

We then assessed uptake of HIV_{JR-FL} NFL TD CC+ trimer-coated beads by THP-1 cells, a human monocyte cell line, as a measure of ADCP (Fig. 3B and D). HIV_{JR-FL} was chosen instead of $SHIV_{SF162P3}$ as there is not currently a structurally stable soluble $SHIV_{SF162P3}$ envelope trimer and the inhibitory concentrations of both bnAbs are comparable for HIV_{JR-FL}. These in vitro studies revealed that PGT121 and b12 were equally effective at binding and inducing ADCP (Fig. 3D).

We hypothesized that there may be differences in glycosylation of b12 and PGT121 because b12 and b12-LALA were produced in Chinese Hamster Ovary cells (ATCC CCL-61) while all PGT121 variants were produced in human embryonic kidney cells (FreeStyle 293-F Cells; fig. S5). Using mass spectrometry, we found higher frequencies of galactosylation in CHO-produced b12. However, we observed similar frequencies of fucosylation across the antibodies and no difference in ADCP in the trimer-coated beads assay between b12 produced in CHO or 293-F cells. These data suggest that alternative glycosylation may not contribute to differences observed in ADCP. However, we observed that 293F-produced b12 displayed lower NK cell killing compared to its CHO-produced counterpart (Fig. 3C and fig S6), suggesting that this slight difference in glycosylation could contribute to differing ADCC activities *(15)*.

Discussion

It has been long known that antibodies can make use of effector functions mediated through Fc receptors as well as neutralization in protection against viruses *(16)*. For example, FcγR effector functions have been shown to be important for protection against alphavirus infection *(17)* and protection by heterosubtypic stem-specific antibodies in the context of influenza A virus infection *(18)*. For HIV, studies with a first generation bnAb in NHPs implied that effector functions could contribute to protection, both in terms of sterilizing immunity and in delaying and reducing the magnitude of primary viremia and morbidity *(1, 2)*. Humanized mouse model studies *(4)* lent support to this view, although the model did not strictly describe prophylactic activity. However, a recent study using a second generation potent bnAb, PGT121, found no evidence for a contribution of effector function to protection from cell-associated virus *(19)*. There were notable differences between that study and the earlier ones, including the route of challenge and form of the challenge virus. In addition, the study was carried out under conditions of high bnAb concentration that may mask contributions of effector functions to protection *(4)*. Concerns have also been expressed that the antibody variant (LALA) typically

used to assess the role of effector functions may not completely eliminate all such functions *(11)*. Accordingly, we carried out an extensive study of PGT121 protection to address some of these questions.

Our central finding is that effector function does not contribute to PGT121 protection against single high-dose vaginal SHIV challenge, even at semi-protective concentrations when effector functions might have the greatest opportunity to contribute. The finding with a high Ab dose was in agreement with that of Parsons et al *(19)*, despite aforementioned differences, and is supported by correlation of protection with day 0 serum neutralizing titers. Further, these findings were confirmed using a variant of PGT121 (LALAPG) in which any residual binding to rhesus FcγRs had been eliminated.

We investigated possible in vitro correlates of the different mechanisms of protection mediated by bnAbs b12 and PGT21, despite limitations associated with in vitro assays. These assays provided no clear indication of a difference between b12 and PGT121 that would explain their distinct protection profiles. It is notable that, in previous studies, b12 was used at much higher doses than PGT121, producing much higher serum Ab concentrations in vivo. Yet, when the ability of PGT121 and b12 to induce ADCC or ADCP were compared in vitro, we found no difference between the bnAbs.

Our study does have some limitations. In order to compare PGT121 with the earlier extensive data on b12 protection, we endeavored to keep similar conditions. The time period between administration of the antibodies and virus challenge was maintained at one day although more recent data indicates that a longer time period may lead to better tissue penetrance of antibody. We also used high-dose virus challenge, again for reasons of consistency, although low-dose repeated challenge may have given better statistical power. However, the low-dose repeated challenge model may be associated with greater macaque anti-human antibody problems. A further limitation, referred to above, is the artificiality of many of the best available effector function assays in attempts to explain differences between antibodies. For instance, antibody phagocytosis of protein-coated beads in vitro may be a very poor predictor of phagocytosis of virions in vivo.

The results described to date suggest it will be difficult to generalize confidently with respect to the contributions of antibody effector function in the context of HIV bnAb-mediated protection. It may well be that the more potent second generation bnAbs are less dependent on effector function than the first generation. Alternatively, the site of vulnerability recognized by the bnAb might be critical. A further possibility is that an Fc-dependent effector activity that is not well modeled by the current in vitro assays is essential for bnAb function. Investigation of protection with more bnAbs is required to definitively distinguish these possibilities. Given current information, it is prudent that clinical passive antibody and HIV vaccine efforts emphasize neutralizing potency while more data is gathered on effector functions.

Methods

Study design

The research aim of this study was to test whether a second generation, highly potent bnAb had the same dependence on effector function for protection as a first generation, less potent bnAb. Another hypothesis was whether a contribution of effector function could be masked by high concentrations of bnAb in vivo. To this end, the impacts of antibody dose or functional knockout mutations (L234A, L235A, with or without P329G) on passive immunization protection of NHPs from SHIV challenge infection were assessed. NHP group sizes were determined in consultation with statisticians to maximize statistical power of group comparisons with the minimum number of animals, resulting in group sizes between 3 (DEN3) and 15 animals (PGT121-LALAPG). For logistic reasons the animal experiments were split into two or three repetitions (IS-35, IS-49, IS-82; IS-108, IS-109). Experiments were terminated after 78 days to ensure delayed infection was appropriately ascertained. Data collection for IS-35, IS-49, and IS-82 were extended for a longer period of time to assess potential vaccinal effects. In addition, animals were euthanized if they showed signs of distress.

Animals

70 adult, female, captive-bred rhesus macaques (*Macaca mulatta*) of Indian origin were obtained from the colonies of Wisconsin National Primate Research Center (WNPRC), or California National Primate Research Center (CNPRC). The median age was 10.3 years (range of 4-21.8 years) with median body weight of 7.66 kg (range of 4.67-14.42 kg). Animals were distributed so MHC-I and FCGR alleles (determined by the Genetics Services unit of the WNPRC) were represented as evenly as possible in the experimental groups.

All animals were cared for at the WNPRC according to Weatherall report guidelines under a protocol approved by the University of Wisconsin - Madison Animal Care and Use Committee and managed according to the research animal husbandry program of the WNPRC. A macaque nutritional plan was closely monitored by animal research technicians and followed the recommendations of the National Research Council (2050 Teklad Global 20% Protein Primate Diet twice daily). The diet was supplemented with a variety of fruits, vegetables, and dairy products as part of the environmental enrichment program.

SHIV-challenged animals were single-housed and twice-daily evaluated for signs of pain, illness, and stress by observing appetite, stool, typical behavior, and physical condition by the staff of the Animal Services Unit. Animals exhibiting distressed behaviors were reported to the Behavioral Management staff and managed accordingly. If any of the above parameters were found to be unacceptable, a member of the WNPRC veterinary staff was notified and their recommendations followed. All efforts were made to minimize suffering.

Intravenous antibody infusion, intravaginal SHIV challenge, and routine blood draws were performed under anesthesia using up to 7 mg/kg ketamine intramuscularly, and up to 0.03 mg/kg dexmedetomidine intramuscularly. Anesthesia was reversed at the conclusion of a procedure by up to 0.3 mg/kg atipamezole intravenously.

Euthanasia was performed at the end of the study or if an animal experienced conditions deemed distressful by one of the veterinarians at the WNPRC. Euthanasia was performed according to the recommendations of the Panel on Euthanasia of the American Veterinary Medical Association (>50 mg/kg of sodium pentobarbital intravenously, preceded by > 15 mg/kg body weight ketamine intramuscularly).

$SHIV_{SF162P3}$ challenge

Macaque menstrual cycles were synchronized with delivery of 30 mg medroxyprogesterone acetate intramuscularly to each animal 28 days before viral challenge to reduce the thickness of the vaginal epithelium for approximately 28-33 days. Lower reproductive tract inflammation may decrease the threshold for virus infection, thus animals received a seven-day course of broad-spectrum antibiotics prior to viral challenge (2.5mg/kg enrofloxacin intramuscularly, twice-daily). Anesthetized animals received 300 $TCID_{50}$ of $SHIV_{SF162P3}$ in the vaginal lumen atraumatically to initiate viral challenge.

Anti-HIV Env monoclonal Antibodies

The HIV bnAbs PGT121 *(7)* and b12 *(22)*, and variants thereof, were expressed in Freestyle 293-F cells (PGT121, Thermo Fisher Scientific), or a stable CHO cell line (b12 variants, *(1)*). Supernatant was harvested after 6-7 days, clarified by centrifugation and filtration through 0.22 µm Rapid-Flow filter units (Nalgene). Antibodies were recovered using Protein G Sepharose Fast Flow (GE Healthcare) in columns, washed with Dulbecco's phosphate buffered saline (DPBS), and eluted with 0.1 M glycine pH 2.5. Antibodies were concentrated and buffer exchanged into DPBS by ultrafiltration. LALA Fc mutations were introduced by site-directed mutagenesis using the Quikchange II mutagenesis kit (Agilent cat. 200523) and the P329G mutation was introduced with the Q5 Site-Directed Mutagenesis Kit (New England BioLabs cat. E0554S) according to the manufacturers' instructions.

Soluble *Env* trimer production

HIV envelope trimers BG505 N332 SOSIP.664 v5.2 *(23)* and JRFL NFL TD CC+ *(24)* containing a C-terminal Avi tag were expressed in Freestlye 293-F cells by co-transfection with furin and purified using PGT145-affinity columns *(25)* and size exclusion chromatography (SEC). Intact trimer fractions were pooled, concentrated to 1–2 mg/ml and sterile filtered prior to aliquoting and freezing at -80°C.

Soluble rhesus FcγR production

The ectodomain genes of Fc gamma receptors from Rhesus Macaques (*Macaca mulatta*) were synthesized fused to a thrombin site, an avi- and a hexa-histidine tags (GeneArt) and cloned into the pcDNA3.4 mammalian expression vector. Proteins were expressed in Freestyle 293-F cells, purified by nickel nitrilotriacetic acid (Ni-NTA) Sepharose and SEC.

Biotinylation of soluble HIV envelope trimers and FcγRs

Avi-tagged recombinant proteins were enzymatically biotinylated using the BirA biotin-protein ligase standard reaction kit (Avidity) according to the manufacturer's instructions.

Pseudovirus and replication competent virus production

$SHIV_{SF162P3}$ envelope pseudotyped virus supernatant from transfected cells was sterile filtered 48-60 hours post transfection, ultra-centrifuged at 100,000 x g for 1 hour, resuspended in DMEM containing 10% fetal bovine serum (FBS) and frozen in aliquots at -80°C *(26)*. Pseudovirus was titrated on TZMbl cells using luciferase expression as readout. Replication competent viruses used in ADCC assays were generated as above using a single plasmid expressing the complete $SHIV_{SF162P3}$ genome transfected in HEK293T cells. Replication competent virus was titrated on CEM.NK^R $CCR5^+Luc^+$.1c12 cells to determine optimal infection and viability for subsequent ADCC assays.

Detection of Env-specific antibodies in serum by ELISA

BG505.SOSIP.N332T-HIS (3µg/ml) in phosphate buffered saline (PBS)/1% bovine serum albumin (BSA)/0.05% Tween 20 (PBS/BT) was bound to ELISA plates pre-coated with anti-His mAb (2µg/ml in PBS) and pre-blocked with PBS/3% BSA, and washed. Sera were heat-inactivated (30 min, 56°C), serially diluted in PBS/BT and allowed to bind to Env-coated plates for 1 hour. After washing, bound serum antibodies were detected using alkaline phosphatase labelled goat anti-human IgG (1:2000 in PBS/BT, 1 hour) and 4-Nitrophenyl phosphate disodium salt substrate with PGT121 as a standard. Non-linear four parameter Hill Curve regression was performed using 450nm optical density (OD) data, Prism 7 and 8 software (Graphpad Software), and logarithmized x-values. Serum dilution giving half-maximal ODs at 450nm (EC_{50}) was determined, and original antibody concentrations were calculated from PGT121 standards. In cases of incomplete titration curves, curve fitting was constrained with top values determined for the PGT121 standards to avoid curve fitting artifacts.

Evaluation of binding of Ig-variants to rhesus FcγRs by ELISA

Antibodies were serially diluted in PBS/1% BSA and allowed to bind to rhesus FcγR (5µg/ml in PBS) pre-coated and blocked (PBS/3% BSA) clear ELISA plates at room temperature for 1 hour. After washing, bound Ig was detected using horseradish peroxidase-labelled $F(ab')_2$ goat-anti human $F(ab')_2$ antibody (Jackson ImmunoResearch, 1:10,000 in PBS/1% BSA, 1 hour) and pre-mixed 3,3',5,5'-Tetramethylbenzidine (TMB)-substrate (Thermo Fisher Scientific). Color reactions were stopped by the addition of 2N sulfuric acid and ODs were determined at 450nm.

Antibody Dependent Bead Phagocytosis (ADBP)

ADBP was performed as described *(20)*. 1µm fluorescein isothiocyanate (FITC) containing neutravidin coated beads (Invitrogen) were incubated with 25 µg/ml enzymatically biotinylated soluble HIV envelope trimer ($HIV_{JR\text{-}FL\ NFL\ TD\ CC+}$) in PBS/0.1% BSA. Antibody aggregates were sedimented immediately prior to the assay by ultracentifugation of endotoxin-free mAbs at 50,000 revolutions per minute (rpm) and 4°C for 15 min in TLA 100.3 rotor (Beckman Coulter). The top 10% of the supernatant volume was then transferred to a new container, and the bnAb concentration was determined by OD_{280} measurement. Beads were washed and incubated in 96 well round bottom plates (Corning) with serial bnAb (b12 or PGT121 and mutants, control DEN3) dilutions in DPBS/0.1% BSA. After 2 hours, 50,000 THP-1 cells were added to the beads and incubated at 37°C, 5% CO_2, 80% humidity for 16-18 hours overnight. Cells were fixed by the addition of an equal volume of 4% formaldehyde, washed with DPBS containing 2% FCS and 1 mM EDTA, and analyzed on a BD FACS Lyric flow cytometer with a universal plate loader. Statistics (FITC mean fluorescence intensity [MFI], % FITC-positive cells) were calculated with FlowJo v10.4.0. The integrated MFI was calculated by multiplying the (% $FITC^+$) x (FITC MFI) and graphed using Graphpad Prism v7.

Antibody Dependent Cellular Cytotoxicity (ADCC)

The CEM.NK^R $CCR5^+Luc^+$ cell line *(14)* was subcloned by limiting dilution and screened for low spontaneous killing by primary human NK cells and high luciferase expression following infection. Subclone 1C12 was used for all subsequent experiments. CEM.NK^R $CCR5^+Luc^+$.1c12 cells were infected with replication competent HIV_{JRFL} or $SHIV_{SF162P3}$. Three days later, target cells were opsonized with serial dilutions of HIV bnAbs or control Abs for 1 hour at 37°C. For NK ADCC assays, thawed human PBMCs from leukapheresis (Stemcell) were allowed to rest overnight in RPMI-1640 (Corning) plus 10% FBS (Omega Scientific), penicillin/streptomycin (Corning), and L-glutamine (Corning) (R10 media) before NK cells were isolated using human NK cell enrichment kits (Stemcell). Purity was confirmed by flow cytometry using fluorescent antibodies to CD14, CD16, and CD56 (BD BioSciences) according to the manufacturer's instructions. 10,800 NK cells at 90 to 95% purity were added to 10,200 infected and opsonized CEM.NK^R $CCR5^+Luc^+$.1c12 cells at a rate of about 20-40% infected. This provided an effector:infected target ratio of 2.4:1 – 5:1. Cells were incubated overnight. KHYG-1 killer assays were performed as described in *(14)*. Uninfected CEM.NK^R $CCR5^+Luc^+$.1c12 cells were used to determine baseline luciferase activity, which was subtracted from all values. Antibody-mediated specific killing of HIV-infected target cells was evaluated by measuring luciferase activity and normalizing to non-specific killing in control wells containing infected target cells co-cultured with effector cells but no HIV-specific Abs. The percent specific killing was calculated as percentage of max luciferase signal in wells with no antibody.

Glycoanalyses by mass spectrometry

Glycoanalyses were performed as described in *(27)*. In brief, 100-150 mg of indicated antibody variants were buffer exchanged using Vivaspin 100 kDa columns, denatured, reduced, and alkylated by sequential 1 hour incubations at room temperature. The proteins were then buffer exchanged into 50 mM Tris/HCl, pH 8.0 using Vivaspin 3 kDa columns and aliquots were

digested with trypsin or chymotrypsin (Mass Spectrometry Grade, Promega) at a ratio of 1:30 (w/w) for 16 hours at 37°C. The reactions were dried and peptides or glycopeptides were extracted using C18 Zip-tip (Merck Millipore) following the manufacturer's protocol. The reaction mixture was loaded onto the tip and eluted with 50% acetonitrile, 0.1% trifluoracetic acid. Eluted peptides and glycopeptides were dried again and re-suspended in 0.1% formic acid prior to mass spectrometry analysis. An aliquot of peptides and glycopeptides was analyzed by liquid chromatography–mass spectrometry (LC-MS) with an Easy-nLC 1200 system coupled to an Orbitrap Fusion mass spectrometer (Thermo Fisher Scientific) using higher energy collisional dissociation (HCD) fragmentation. Peptides and glycopeptides were separated using an EasySpray PepMap RSLC C18 column (75 mm x 75 cm) with a 275 min. linear gradient consisting of 0%–32% acetonitrile in 0.1% formic acid over 240 minutes followed by 35 minutes of 80% acetonitrile in 0.1% formic acid. The flow rate was set to 200 nL/min. The spray voltage was set to 2.8 kV and the temperature of the heated capillary was set to 275°C. HCD collision energy was set to 50%. Byonic (Version 2.7) and Byologic software (Version 2.3; Protein Metrics Inc.) extracted data evaluated manually and each peptide was scored as true-positive when the correct b and y fragment ions were observed along with oxonium ions corresponding to the glycan identified. The relative abundance of unoccupied versus glycosylated sites was calculated using the extracted ion chromatograms for the true-positive peptides.

$SHIV_{SF162P3}$ viral load quantitation

Viral RNA was isolated from plasma samples using the Maxwell 16 Viral Total Nucleic Acid Purification kit on the Maxwell 48RSC instrument (Promega) and quantified using a highly sensitive QRT-PCR assay (limit of detection 100 copies/ml) as previously described *(28)*. Primer and probe sequences included: forward primer: 5'- GTCTGCGTCATCTGGTGCATTC, reverse primer: 5'-CACTAGCTGTCTCTGCACTATGTGTTTTG-3' and probe: 5'-6-carboxyfluorescein-CTTCCTCAGTGTGTTTCACTTTCTCTTCTGCG-BHQ1-3'. Reactions were cycled at 37°C for 15 min, 50°C for 30 min, 95°C for 2 min followed by 50 cycles of 95°C for 15 seconds and 62°C for 1 min.

Neutralization assays

NHP serum collected at various timepoints after passive-immunization was heat inactivated (30 min, 56°C) and incubated for 1 hour at 37°C with pseudovirus, then transferred onto TZM-bl cells (10,000/well) in 96 well plates, in complete DMEM supplemented with 10% FBS (Omega Scientific), penicillin/streptomycin (Corning), L-glutamate (Corning), and 20 µg/mL Diethylaminoethyl (DEAE)-dextran. Supernatant was removed after a 48 hour incubation at 37°C, 5% CO_2, 80% humidity and the cells lysed with lysis buffer (25mM Glycylglycine, 15mM $MgSO_4$, 4mM EGTA tetrasodium salt, 5 ml/L Triton X) for 5 min at room temperature. Luciferase activity was measured by the addition of Bright-Glo luciferase-substrate (Promega), and the luminescence signal read using a BioTek Synergy 2 plate reader. Uninfected cells were used to correct for background luciferase expression.

$CD8^+$ lymphocyte depletion

CD8α-expressing lymphocytes were transiently depleted in vivo by intravenous injection of the anti-CD8α monoclonal antibody (clone M-T807R1) in a single dose of 50 mg/kg of body weight. The antibody was provided by the National Institutes of Health Nonhuman Primate Reagent Resource, lot number LH16-12. The efficacy of CD8α depletion was monitored by flow cytometry.

Rhesus macaque MHC-I tetramer staining

Mamu-A*02, Mamu-B*08, and Mamu-B*17 MHC-I tetramers labelled with phycoerythrin (PE), allophycocyanin (APC), or Brilliant Violet (BV)-421 and bound to indicated SIV peptides used to quantify SIV-specific $CD8^+$ T cells as described previously *(29)*. All macaque MHC-I tetramers utilized in this study were obtained from the NIH Tetramer Core Facility. Approximately 800,000 PBMC were incubated in R10 medium with titrated amounts of each tetramer at room temperature for 45 min. Before adding the Mamu-B*17 tetramers to the respective tubes, the cells were pre-incubated with 50 nM of the protein kinase inhibitor Dasatinib for 30 min in order to improve tetramer staining. Following the 45 min tetramer incubation, cells were stained with fluorochrome-labeled mAbs directed against lineage markers CD3 (clone SP34-2; PerCP Cy5.5), CD8α (clone RPA-T8; BV785), CD14 (clone M5E2; BV510), CD16 (clone 3G8; BV510), and CD20 (clone 2H7; BV510) for 25 min at room temperature. A viability marker (ARD; Live/DEAD Fixable Aqua Dead Cell Stain; Life Technologies) was also included in this step (1:4,000 dilution of master stock prepared according to manufacturer's instruction). Cells were washed with Wash Buffer (Dulbecco's PBS with 0.1% BSA and 0.45 g/L NaN_3) and fixed with PBS/2% paraformaldehyde (PFA) for 20 min at 4°C. Next, cells were washed and analyzed on a Special-Order BD LSRII flow cytometer equipped with 50-mW 405-nm (violet), 100-mW 488-nm (blue), and 30-mW 635-nm (red) lasers with FACSDIVA v6 software.

Data was gated on diagonally clustered singlets in height-vs-area plots for forward scatter height (FSC-H/FSC-A) and side scatter (SSC-H/SSC-A) in FlowJo. Singlets were further gated using a time gate between the 5^{th} and 90^{th} percentiles. T lymphocytes were selected as "Dump channel negative" (ARD^-, $CD14^-$, $CD16^-$, $CD20^-$) and $CD3^+$ cells and the lymphocyte population was delineated based on FSC-A/SSC-A properties. Gates were then created to identify $CD8^+$ cells and $tetramer^+$ cells. All tetramer frequencies shown in this study correspond to percentages of live $CD3^+$ $CD8^+$ $tetramer^+$ lymphocytes.

Intracellular cytokine staining (ICS) assay.

Frozen PBMCs were thawed, transferred to 37°C warm R10 medium, and pelleted at 530 x g for 5 min. The pellet was resuspended in R10 and centrifugation was repeated. Pools of peptides (15mers overlapping by 11 amino acids) spanning the SIVmac239 Gag, Vif, and Nef proteins were used for T cell stimulation. Peptides corresponding to SIV epitopes restricted by Mamu-

B*08 were also used for T cell stimulation. The Gag peptides were split into two pools covering amino acids 1-263 or 248-510. The Vif (amino acids 1-214) and Nef (amino acids 1-263) peptides were each grouped into a separate pool. The final assay concentration of each 15mer was 1.0 µM. PBMCs were stimulated with the appropriate pools of SIVmac239 peptides in R10 containing co-stimulatory mAbs against CD28 (clone L293; BD Biosciences) and CD49d (clone 9F10; BD Pharmingen) for 9 hours at 37°C/5.0% CO_2. A PE-conjugated mAb against CD107a (clone H4A3; PE; Biolegend) was also included in this step. Brefeldin A (BioLegend) and GolgiStop (BD Biosciences) were added to all tubes after 1 hour to inhibit protein transport. The tubes were refrigerated at 4°C at the end of this 9 hour incubation. The surface staining was performed as described above, using the same ARD and mAbs against CD14, CD16, CD20. The surface staining mAb cocktail also included mAbs against CD4 (clone OKT4; BioLegend) and CD8 (clone RPA-T8; BioLegend). After the cells were fixed in 2% PFA, they were permeabilized by homogenization in "Perm Buffer" (1× BD FACS lysing solution 2 (Beckton Dickinson) and 0.05% Tween-20 [Sigma-Aldrich]) for 10 min and then washed with Wash Buffer. Cells were then incubated with mAbs against CD3 (clone SP34-2), interferon γ (IFN-γ; clone 4S.B3), tumor necrosis factor-α (TNF-α; clone mAb11), and CD69 (clone FN50) for 1 hour in the dark at room temperature. Lastly, the cells were washed and then stored at 4 °C until analysis by flow cytometry.

After gating on live $CD14^-$ $CD16^-$ $CD20^-$ $CD3^+$ lymphocytes as described above, subsets were analyzed based on their exclusive expression of either CD4 or CD8. Responses were considered positive if they co-expressed IFN-γ and TNF-α. Leukocyte activation cocktail (LAC; BD Pharmingen)–stimulated cells stained with fluorochrome-labeled control mAbs of the same isotypes as those against IFN-γ and TNF-α guided identification of positive populations. Calculations were performed in Microsoft Excel and results were presented as percentages of IFN-γ^+ TNF-α^+ $CD4^+$ or $CD8^+$ T cells.

Cell lines

TZM-bl cells (human female HeLa-derived cancer cell line) and HEK293T cells (human embryonic kidney cancer cell line expressing the SV40 large T antigen) were maintained at 37°C and 5% CO_2 in high glucose Dulbecco's Modified Eagle Medium (DMEM, Corning) containing 1X Penicillin-Streptomycin (Corning), 2 mM L-Glutamine (Corning), and 10% heat-inactivated FBS Omega Scientific. FreeStyle 293F cells (Thermo Fisher Scientific) were maintained at 37°C, 80% humidity, and 8% CO_2 in shaking incubators set to 135 revolutions per minute in serum and antibiotic free FreeStyle 293 Expression Medium (Thermo Fisher Scientific). CEM.NK^R $CCR5^+Luc^+$ cell line derivatives were propagated in RPMI-1640 medium supplemented heat-inactivated 10% fetal bovine serum (FBS, Omega Scientific), 25 mM HEPES (Invitrogen), 2 mM L-glutamine (Invitrogen) and 0.1 mg/ml Primocin (InvivoGen). KGHY-1 rhCD16 cells were cultivated the same way as CEM.NKR.CCR5+Luc+ cells with the addition of 10U/ml interleukin-2 (AIDS Research and Reference Reagent Program) and cyclosporine A (Sigma) at 1 µg per ml.

Statistical Analysis

Data was plotted using Prism 7 and 8 (GraphPad Software), or using custom Python scripts based on the Pandas or Seaborn data analysis packages. Statistical analyses were performed in R and included two sample t tests to assess significance of differences between animal groups in terms of protection, logarithmized AUC, day 0 serum ELISA and neutralization titers. Data and scripts used for these analyses have been deposited online (doi: 10.5281/zenodo.4474217).

List of Supplementary Materials:

References

1. A. J. Hessell, L. Hangartner, M. Hunter, C. E. G. Havenith, F. J. Beurskens, J. M. Bakker, C. M. S. Lanigan, G. Landucci, D. N. Forthal, P. W. H. I. Parren, P. A. Marx, D. R. Burton, Fc receptor but not complement binding is important in antibody protection against HIV, *Nature* **449**, 101–104 (2007).
2. A. J. Hessell, P. Poignard, M. Hunter, L. Hangartner, D. M. Tehrani, W. K. Bleeker, P. W. H. I. Parren, P. A. Marx, D. R. Burton, Effective, low-titer antibody protection against low-dose repeated mucosal SHIV challenge in macaques, *Nat. Med.* **15**, 951–954 (2009).
3. B. Moldt, N. Schultz, D. C. Dunlop, M. D. Alpert, J. D. Harvey, D. T. Evans, P. Poignard, A. J. Hessell, D. R. Burton, A panel of IgG1 b12 variants with selectively diminished or enhanced affinity for Fcγ receptors to define the role of effector functions in protection against HIV, *J. Virol.* **85**, 10572–10581 (2011).
4. S. Bournazos, F. Klein, J. Pietzsch, M. S. Seaman, M. C. Nussenzweig, J. V. Ravetch, Broadly neutralizing anti-HIV-1 antibodies require Fc effector functions for in vivo activity, *Cell* **158**, 1243–1253 (2014).
5. M. Asokan, R. S. Rudicell, M. Louder, K. McKee, S. O apos Dell, G. Stewart-Jones, K. Wang, L. Xu, X. Chen, M. Choe, G. Chuang, I. S. Georgiev, M. G. Joyce, T. Kirys, S. Ko, A. Pegu, W. Shi, J. P. Todd, Z. Yang, R. T. Bailer, S. Rao, P. D. Kwong, G. J. Nabel, J. R. Mascola, G. Silvestri, Ed. Bispecific Antibodies Targeting Different Epitopes on the HIV-1 Envelope Exhibit Broad and Potent Neutralization, *J. Virol.* **89**, 12501–12512 (2015).
6. P. Wang, M. R. Gajjar, J. Yu, N. N. Padte, A. Gettie, J. L. Blanchard, K. Russell-Lodrigue, L. E. Liao, A. S. Perelson, Y. Huang, D. D. Ho, Quantifying the contribution of Fc-mediated effector functions to the antiviral activity of anti-HIV-1 IgG1 antibodies in vivo, *Proc. Natl. Acad. Sci. U.S.A.* **117**, 18002–18009 (2020).
7. L. M. Walker, M. Huber, K. J. Doores, E. Falkowska, R. Pejchal, J.-P. Julien, S.-K. Wang, A. Ramos, P.-Y. Chan-Hui, M. Moyle, J. L. Mitcham, P. W. Hammond, O. A. Olsen, P. Phung, S. Fling, C.-H. Wong, T. Wrin, M. D. Simek, P. G. P. Investigators, W. C. Koff, I. A. Wilson, D. R. Burton, P. Poignard, Broad neutralization coverage of HIV by multiple highly potent antibodies, *Nature* **477**, 466–470 (2011).
8. S. Mahomed, N. Garrett, E. Capparelli, C. Baxter, N. Y. Zuma, T. Gengiah, D. Archary, P. Moore, N. Samsunder, D. H. Barouch, J. Mascola, J. Ledgerwood, L. Morris, S. Abdool Karim, Assessing the safety and pharmacokinetics of the monoclonal antibodies, VRC07-523LS and PGT121 in HIV negative women in South Africa: study protocol for the CAPRISA 012A randomised controlled phase I trial, *BMJ Open* **9**, e030283 (2019).
9. M. S. Parsons, S. B. Lloyd, W. S. Lee, A. B. Kristensen, T. Amarasena, Center, Rob J, B. F. Keele, J. D. Lifson, C. C. LaBranche, D. Montefiori, B. D. Wines, P. M. Hogarth, K. M. Swiderek, V. Venturi, M. P. Davenport, S. J. Kent, Partial efficacy of a broadly neutralizing antibody against cell-associated SHIV infection, *Sci. Transl. Med.* **9**, eaaf1483 (2017).
10. B. Moldt, E. G. Rakasz, N. Schultz, P.-Y. Chan-Hui, K. Swiderek, K. L. Weisgrau, S. M. Piaskowski, Z. Bergman, D. I. Watkins, P. Poignard, D. R. Burton, Highly potent HIV-specific antibody neutralization in vitro translates into effective protection against mucosal SHIV challenge in vivo, *Proc. Natl. Acad. Sci. U.S.A.* **109**, 18921–18925 (2012).

11. T. Schlothauer, S. Herter, C. F. Koller, S. Grau-Richards, V. Steinhart, C. Spick, M. Kubbies, C. Klein, P. Umaña, E. Mössner, Novel human IgG1 and IgG4 Fc-engineered antibodies with completely abolished immune effector functions, *Protein Engineering Design and Selection* **29**, 457–466 (2016).
12. Y. Nishimura, R. Gautam, T. W. Chun, R. Sadjadpour, K. E. Foulds, M. Shingai, F. Klein, A. Gazumyan, J. Golijanin, M. Donaldson, O. K. Donau, R. J. Plishka, A. Buckler-White, M. S. Seaman, J. D. Lifson, R. A. Koup, A. S. Fauci, M. C. Nussenzweig, M. A. Martin, Early antibody therapy can induce long-lasting immunity to SHIV, *Nature* **543**, 559–563 (2017).
13. M. Lo, H. S. Kim, R. K. Tong, T. W. Bainbridge, J.-M. Vernes, Y. Zhang, Y. L. Lin, S. Chung, M. S. Dennis, Y. J. Y. Zuchero, R. J. Watts, J. A. Couch, Y. G. Meng, J. K. Atwal, R. J. Brezski, C. Spiess, J. A. Ernst, Effector-attenuating Substitutions That Maintain Antibody Stability and Reduce Toxicity in Mice, *J. Biol. Chem.* **292**, 3900–3908 (2017).
14. M. D. Alpert, L. N. Heyer, D. E. J. Williams, J. D. Harvey, T. Greenough, M. Allhorn, D. T. Evans, A novel assay for antibody-dependent cell-mediated cytotoxicity against HIV-1- or SIV-infected cells reveals incomplete overlap with antibodies measured by neutralization and binding assays, *J. Virol.* **86**, 12039–12052 (2012).
15. M. Thomann, K. Reckermann, D. Reusch, J. Prasser, M. L. Tejada, Fc-galactosylation modulates antibody-dependent cellular cytotoxicity of therapeutic antibodies, *Mol. Immunol.* **73**, 69–75 (2016).
16. P. W. Parren, D. R. Burton, The antiviral activity of antibodies in vitro and in vivo, *Adv. Immunol.* **77**, 195–262 (2001).
17. J. T. Earnest, K. Basore, V. Roy, A. L. Bailey, D. Wang, G. Alter, D. H. Fremont, M. S. Diamond, Neutralizing antibodies against Mayaro virus require Fc effector functions for protective activity, *J. Exp. Med.* **216**, 2282–2301 (2019).
18. D. J. DiLillo, G. S. Tan, P. Palese, Broadly neutralizing hemagglutinin stalk-specific antibodies require FcγR interactions for protection against influenza virus in vivo, *Nat. Med.* **20**, 143–151 (2014).
19. M. S. Parsons, W. S. Lee, A. B. Kristensen, T. Amarasena, G. Khoury, A. K. Wheatley, A. Reynaldi, B. D. Wines, P. M. Hogarth, M. P. Davenport, S. J. Kent, Fc-dependent functions are redundant to efficacy of anti-HIV antibody PGT121 in macaques, *J. Clin. Invest.* **129**, 182–191 (2019).
20. E. G. McAndrew, A.-S. Dugast, A. F. Licht, J. R. Eusebio, G. Alter, M. E. Ackerman, Determining the phagocytic activity of clinical antibody samples, *J Vis Exp*, e3588 (2011).
21. A. Wyrzucki, C. Dreyfus, I. Kohler, M. Steck, I. A. Wilson, L. Hangartner, Alternative recognition of the conserved stem epitope in influenza A virus hemagglutinin by a VH3-30-encoded heterosubtypic antibody, *J. Virol.* **88**, 7083–7092 (2014).
22. P. Roben, J. P. Moore, M. Thali, J. Sodroski, C. F. Barbas, D. R. Burton, Recognition properties of a panel of human recombinant Fab fragments to the CD4 binding site of gp120 that show differing abilities to neutralize human immunodeficiency virus type 1, *J. Virol.* **68**, 4821–4828 (1994).
23. A. Torrents de la Peña, J.-P. Julien, S. W. de Taeye, F. Garces, M. Guttman, G. Ozorowski, L. K. Pritchard, A.-J. Behrens, E. P. Go, J. A. Burger, E. E. Schermer, K. Sliepen, T. J. Ketas, P. Pugach, A. Yasmeen, C. A. Cottrell, J. L. Torres, C. D. Vavourakis, M. J. van Gils, C. LaBranche, D. C. Montefiori, H. Desaire, M. Crispin, P.-J. Klasse, K. K. Lee, J. P. Moore, A. B. Ward, I. A.

Wilson, R. W. Sanders, Improving the Immunogenicity of Native-like HIV-1 Envelope Trimers by Hyperstabilization, *Cell Rep* **20**, 1805–1817 (2017).
24. J. Guenaga, F. Garces, N. de Val, R. L. Stanfield, V. Dubrovskaya, B. Higgins, B. Carrette, A. B. Ward, I. A. Wilson, R. T. Wyatt, Glycine Substitution at Helix-to-Coil Transitions Facilitates the Structural Determination of a Stabilized Subtype C HIV Envelope Glycoprotein, *Immunity* **46**, 792–803.e3 (2017).
25. P. Pugach, G. Ozorowski, A. Cupo, R. Ringe, A. Yasmeen, N. de Val, R. Derking, H. J. Kim, J. Korzun, M. Golabek, K. de Los Reyes, T. J. Ketas, J.-P. Julien, D. R. Burton, I. A. Wilson, R. W. Sanders, P. J. Klasse, A. B. Ward, J. P. Moore, R. W. Doms, Ed. A native-like SOSIP.664 trimer based on an HIV-1 subtype B env gene, *J. Virol.* **89**, 3380–3395 (2015).
26. M. Pauthner, C. Havenar-Daughton, D. Sok, J. P. Nkolola, R. Bastidas, A. V. Boopathy, D. G. Carnathan, A. Chandrashekar, K. M. Cirelli, C. A. Cottrell, A. M. Eroshkin, J. Guenaga, K. Kaushik, D. W. Kulp, J. Liu, L. E. McCoy, A. L. Oom, G. Ozorowski, K. W. Post, S. K. Sharma, J. M. Steichen, S. W. de Taeye, T. Tokatlian, A. Torrents de la Peña, S. T. Butera, C. C. LaBranche, D. C. Montefiori, G. Silvestri, I. A. Wilson, D. J. Irvine, R. W. Sanders, W. R. Schief, A. B. Ward, R. T. Wyatt, D. H. Barouch, S. Crotty, D. R. Burton, Elicitation of Robust Tier 2 Neutralizing Antibody Responses in Nonhuman Primates by HIV Envelope Trimer Immunization Using Optimized Approaches, *Immunity* **46**, 1073–1088.e6 (2017).
27. G. E. Seabright, C. A. Cottrell, M. J. van Gils, A. D'addabbo, D. J. Harvey, A.-J. Behrens, J. D. Allen, Y. Watanabe, N. Scaringi, T. M. Polveroni, A. Maker, S. Vasiljevic, N. de Val, R. W. Sanders, A. B. Ward, M. Crispin, Networks of HIV-1 Envelope Glycans Maintain Antibody Epitopes in the Face of Glycan Additions and Deletions, *Structure/Folding and Design*, 1–20 (2020).
28. A. N. Cline, J. W. Bess, M. Piatak, J. D. Lifson, Highly sensitive SIV plasma viral load assay: practical considerations, realistic performance expectations, and application to reverse engineering of vaccines for AIDS, *Journal of Medical Primatology* **34**, 303–312 (2005).
29. L. Gonzalez-Nieto, A. Domingues, M. Ricciardi, M. J. Gutman, H. S. Maxwell, N. Pedreño-Lopez, V. Bailey, D. M. Magnani, M. A. Martins, Analysis of Simian Immunodeficiency Virus-specific CD8+ T-cells in Rhesus Macaques by Peptide-MHC-I Tetramer Staining, *J Vis Exp*, e54881 (2016).
30. Y. Watanabe, S. Vasiljevic, J. D. Allen, G. E. Seabright, H. M. E. Duyvesteyn, K. J. Doores, M. Crispin, W. B. Struwe, Signature of Antibody Domain Exchange by Native Mass Spectrometry and Collision-Induced Unfolding, *Anal. Chem.* **90**, 7325–7331 (2018).

Acknowledgements

We thank Javier Guenaga for providing the JRFL NFL TD CC+ construct, and Matteo Bianchi for the BG505 N332 SOSIP v5.2 construct. We are grateful to the WNPRC Genetics Services, Roger Wiseman and his team, for performing all haplotyping. We thank Diane Kubrik from the Center for Antibody Development and Production at The Scripps Research Institute for producing all antibodies used in vivo and David Evans for providing the CEM.NK^{R}-CCR5-Luc and KHYG cell lines used in this study.

Funding

This work was funded by NIH grants 5R37 A1055332 and UM1AI100663 to DRB and UM1AI144462 to DRB and LH. The Swiss National Science Foundation Fellowship P2ZHP3_174834 supported DB. This nonhuman primate study was performed at the Wisconsin National Primate Research Center supported in part by NCRR grant P51OD011106. MAM was supported by K01 0D023032 from the Office of the Director, NIH.

Author contributions

LH designed and planned the study in collaboration with DRB. DB planned, conducted and supervised in vitro experiments. ER was in charge of all in vivo animal work performed for this study. Technical assistance to LH and DB was provided by RN and KM. Statistical power calculations for experimental planning of NHP experiments were conducted by NH and RRR, statistical analyses of experimental data was performed by NH, and CTL responses were evaluated by MAM. Glycoanalyses were performed by GES, JDA and MC, AMW and TCF determined viral titers. The manuscript was prepared by LH, DB and DRB. All authors reviewed and agreed on the final version.

Competing interests

DRB is a joint holder of a patent on PGT121 (WO2012030904A2 - Human immunodeficiency virus (HIV)-neutralizing antibodies). Dr. Martins has a consulting financial interest in Emmune, Inc., a company that is developing HIV immunotherapies based on the immunoadhesin eCD4-Ig. All other authors have no other conflicting interests to declare.

Data Availability

All data associated with this study are in the paper or deposited on Zenodo (doi: 10.5281/zenodo.4474217).

Figures Legends

Figure 1. Macaques are equally protected against single high-dose vaginal challenge with $SHIV_{SF162P3}$ by transfer of 1mg/kg of PGT121 or PGT121-LALA. Viral loads after $SHIV_{SF162P3}$ challenge following passive transfer of PGT121, PGT121-LALA, or a control antibody, DEN3. Animal groups were balanced for weight, FcγR and MHC alleles, and their menstrual cycles were synchronized by administration of DepoProvera 30 days before infection. Daily Benadryl antibiotic application courses were initiated on day -7 to treat latent vaginal infections or inflammation. Indicated antibodies were then infused intravenously one day before intravaginal administration of 300 $TCID_{50}$ of $SHIV_{SF162P3}$. Animal identifications are listed in the symbol legend, open symbols represent infected animals, closed symbols denote protected animals. Dashed lines indicate the assay limit of detection.

Figure 2 Macaques are equivalently protected against single high-dose vaginal challenge with $SHIV_{SF162P3}$ following administration of 0.2mg/kg of PGT121 or PGT121-LALA. Animals were prepared as in Fig. 1. Low doses of antibodies (0.2mg/kg) were infused intravenously one day before intravaginal administration of 300 $TCID_{50}$ of $SHIV_{SF162P3}$. Viral titers are shown for each of the three experiments (IS-35, IS-49 and IS-82; columns). Animal identifications are listed in the symbol legend, open symbols represent infected animals, closed symbols denote protected animals. Symbols in yellow indicate three IS-82 animals that were found to be Chinese/Indian hybrid animals during major histocompatibility complex genotyping (rh2540, rh2541, rh2544).

Figure 3. Differences in effector function activities of PGT121 and b12 fail to provide an explanation for their differing in vivo behaviour (A) Graphs indicate binding of Fc-variants of PGT121 to recombinantly expressed rhesus FcγRs. Plates were coated with recombinant soluble FcγR at 5µg/ml before titrated amounts of the indicated antibodies were allowed to bind. Bound antibodies were then detected by peroxidase labelled $F(ab')_2$ anti-human $F(ab')_2$. Mean and SD from two technical replicates are displayed. OD: optical density **(B)** THP-1 cell phagocytosis of $HIV_{JR\text{-}FL}$ envelope coated beads was compared across PGT121 and b12 and mutants. Titrated amounts of both the wild-type and effector-crippled version of the indicated ultracentifuged bnAbs were used to opsonize $HIV_{JR\text{-}FL\ NFL\ TD\ CC+}$ trimer-coated 1 µm fluorescent beads. THP-1 cells were then added to antibody and bead mixtures and incubated overnight at 37°C. Opsonization was evaluated by flow cytometry and the integrated mean fluorescence intensity (iMFI) was calculated. Data represents mean and SD from two replicates, gray areas indicate the PGT121 serum concentration range in the NHP protection experiments. **(C)** NK cell-mediated ADCC activities of b12 and PGT121 were compared in vitro. $SHIV_{SF162P3}$ -infected $CEM.NK^{R}.CCR5^{+}Luc^{+}.1c12$ cells were incubated with the indicated antibodies and then used as target for KHYG-rhCD16 cells (left) or primary human NK cells (right). The donor ID for the human NK cells is indicated above the panel. Data represents mean and SD from two replicates. **(D)** THP-1 cell binding and phagocytosis of $HIV_{JR\text{-}FL\ NFL}$ coated beads was evaluated at concentrations reflective of in vivo challenge studies. Data represent mean and standard deviation from 4 independent experiments. Anti-influenza HA mAb 3.1 *(21)* was used as a negative control and data represent two replicates. Light and dark gray areas indicate the

serum concentration range of the respective PGT121 and b12 antibodies in the relevant NHP protection experiments.

Figure 4. PGT121-LALAPG variant is equivalently protective as PGT121 or PGT121-LALA. (A) Viral loads after single high-dose $SHIV_{SF162P3}$ vaginal challenge following transfer of 0.2mg/kg of the indicated antibody are plotted (experiment IS-108/109). Antibodies (0.2mg/kg) were infused intravenously one day before intravaginal administration of 300 $TCID_{50}$ of $SHIV_{SF162P3}$. Animal identifications are listed in the symbol legend, open symbols represent infected animals, closed symbols denote protected animals. Dashed lines indicate the limit of detection of the assay. **(B)** Meta-analysis of viremia in break-through animals. Area under the curve values were integrated for viremic animals from day 0 though day 77 post infection. Data is displayed as individual values (gray dots), mean (central line) interquartile range (box) and minimum to maximum range (whiskers). Indicated p values were determined by Welch two sample t-tests.

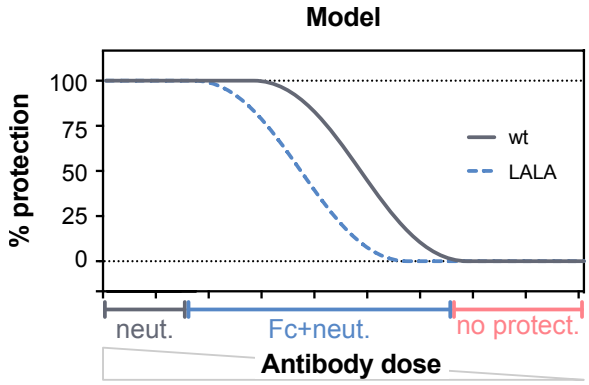

Fig. S1. Hypothesis for possible effector function augmentation in relation to antibody concentration.

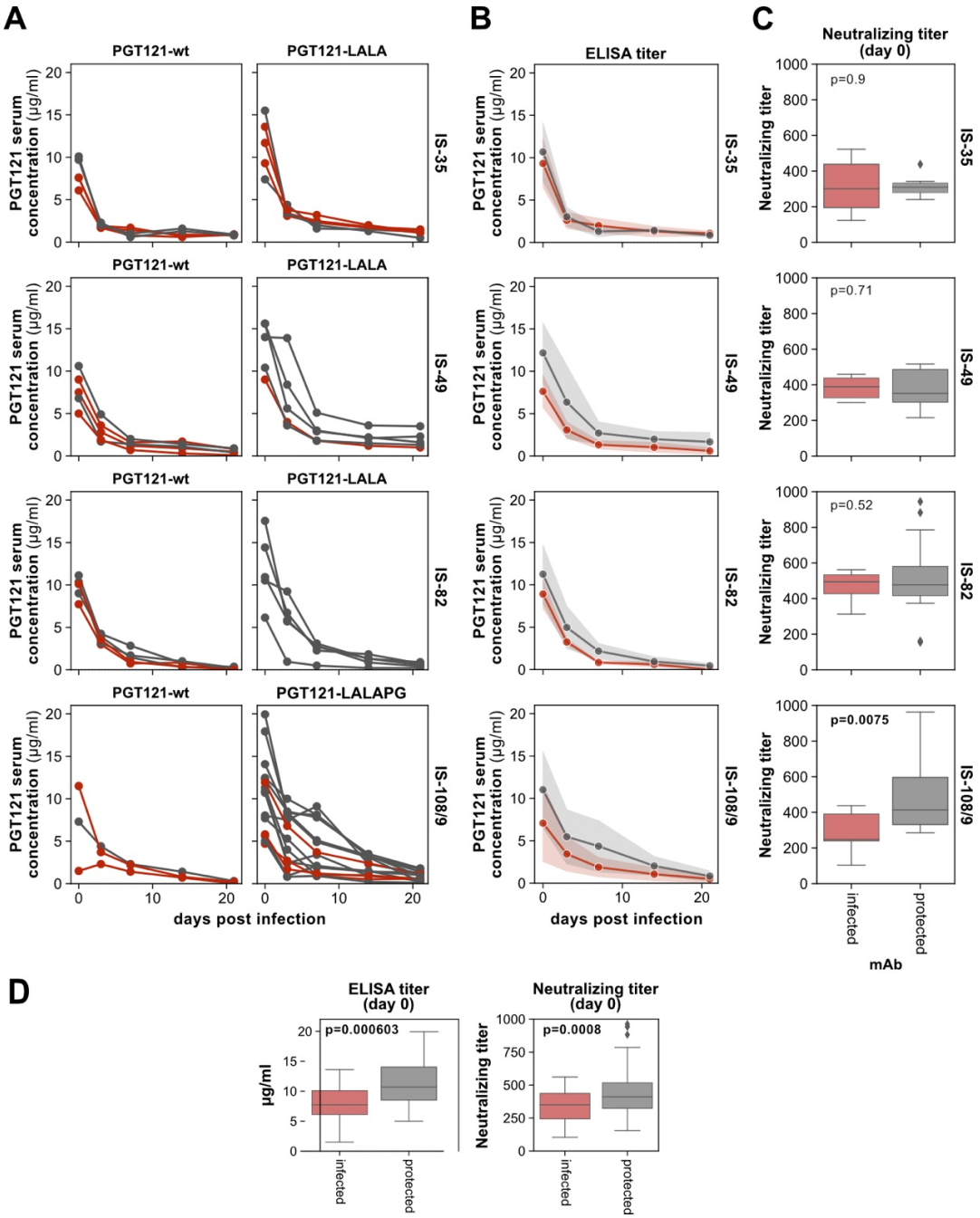

Fig. S2. PGT121 serum antibody titers. (A) Individual macaque PGT121 serum concentrations were measured over time. HIV-specific IgG was detected by ELISA and EC_{50} values were determined using non-linear regression and translated into concentrations using wild type (wt) PGT121 standards. Protected animals are indicated in gray, infected animals that were viremic at any point are indicated in red. **(B)** Serum concentrations were compared between wild-type and Fc-crippled variants displayed in (A) binned by the outcome of the challenge, and plotted as mean values over time with the corresponding standard deviation indicated as a semi-transparent band. **(C)**

$SHIV_{SF162P3}$ pseudovirus serum neutralizing titers on the day of infection were evaluated and binned by outcome. Data were plotted as median (line) interquartile (box) and 1.5x interquartile range (whiskers). Outliers are indicated as diamonds and indicated p values were determined by Welch two sample t-tests. **(D)** Day 0 ELISA and neutralizing antibody titers were plotted by outcome. Data from B and C were binned according to outcome and plotted as above. Indicated p values were determined by Welch two sample t-tests.

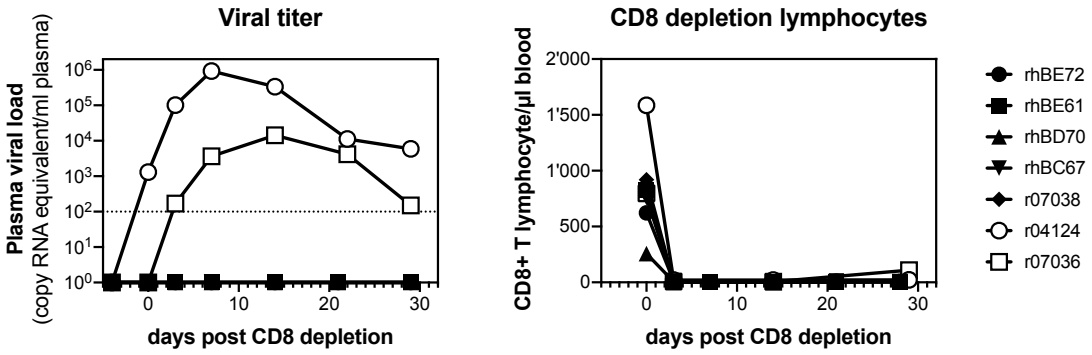

Fig. S3. CD8 depletion to probe presence of virus in antibody-treated macaques. Blood viremia (left panel) was quantified following depletion of $CD8^+$ T cells. Animals had previously received wild-type or LALA PGT121 and either remained uninfected (bold face symbols) or became infected and spontaneously controlled viremia. 482 days post infection, $CD8^+$ T cells were depleted by a single injection of 50 mg/kg of mAb cM-T807 on day 0. Successful depletion of $CD8^+$ cells was confirmed 3 days post treatment by flow cytometry (right panel).

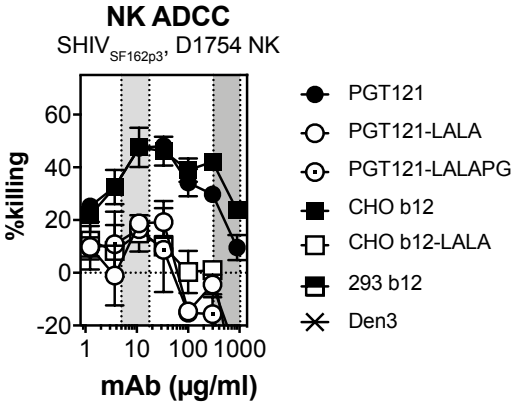

Fig. S4. Additional in vitro ADCC assay. Human NK cell ADCC (donor D1754) was measured in vitro with Ab concentrations up to those measured in passive immunization experiments. Light and dark gray areas indicate the serum concentration range present on day 0 in PGT121 and b12 protection experiments, respectively**.**

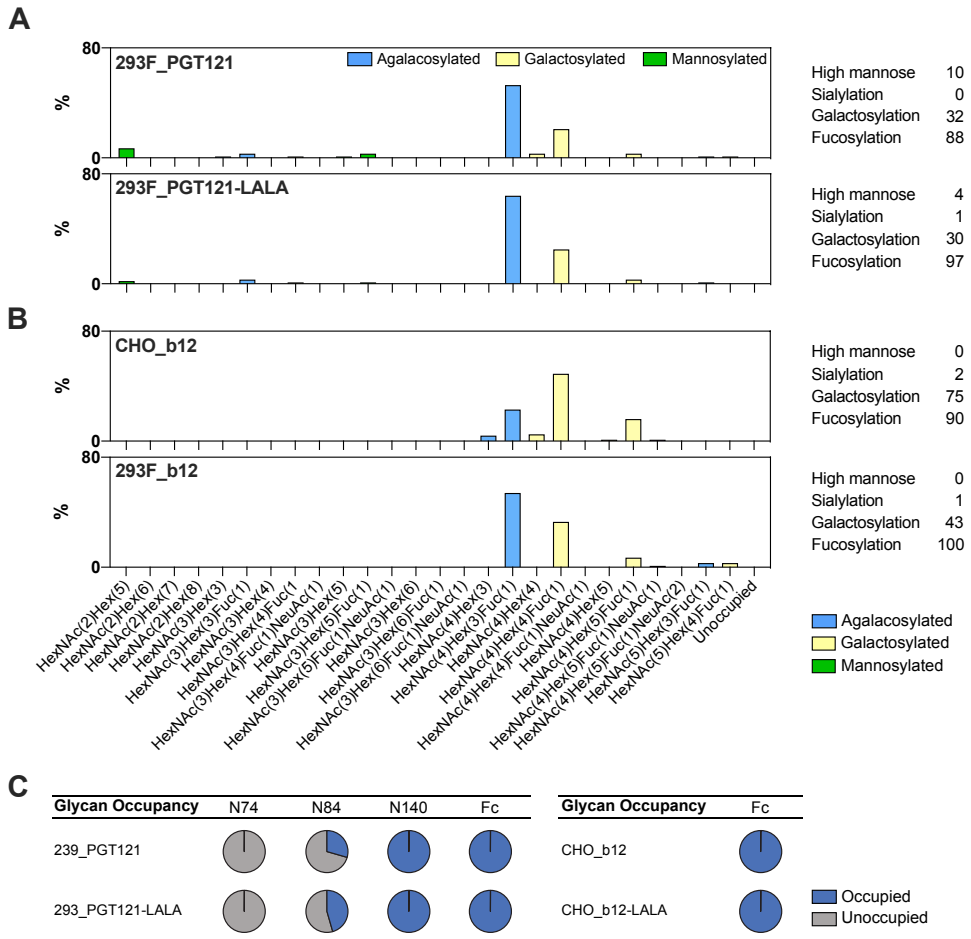

Fig. S5. Glycoanalyses of CHO-produced b12 and 293F cell-produced PGT121 variants. Antibody glycosylation and occupancy was determined using liquid chromatography-mass spectrometry (LC-MS). The PGT121 heavy chain contains 4 glycosylation sites, three sites in the Fab region (N74, N84 and N140) and one in the Fc, while b12 contains just the Fc site. **(A)** Relative quantification of glycosylation present on the Fc glycan of PGT121 produced in HEK293F, and impact of LALA mutation. The different glycan compositions detected across all antibodies are shown on the x-axis. Hex refers to a hexose monosaccharide and HexNAc refers to a hexosamine monosaccharide. LALA mutations had only a small impact upon Fc glycosylation. **(B)** Relative quantification of glycosylation present on the Fc glycan of b12 produced in CHO and HEK 293F cells. CHO-expressed b12 displayed a glycosylation pattern that differed from that observed on PGT121. **(C)** Occupancy of glycosylation sites. The relative chromatographic areas were compared for a single peptide sequence with different post translational modifications to determine the proportion of N-linked glycan sites occupied and those lacking a glycan. Unoccupied peptides could not be detected for N140 and for the conserved Fc glycan site. No unoccupied peptides were detected for b12 expressed in CHO cells with or without LALA mutations.

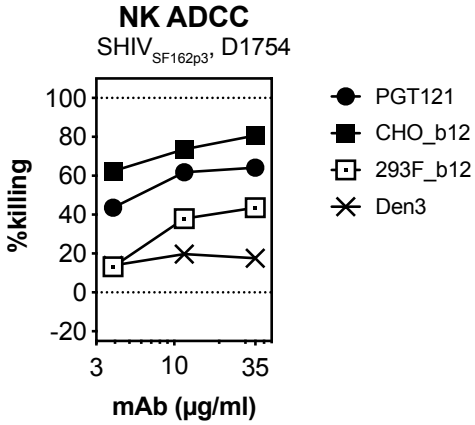

Fig. S6. Effect of producer cell line on ADCC activity. Human NK ADCC activity (donor D1754) against $SHIV_{SF162p3}$ infected target cells was measured using mAbs produced in the indicated cell lines.

Table S1. Assessment of T cell priming in protected animals. Using frozen peripheral blood mononuclear cells and the assays indicated, the presence of T cells specific for the indicated epitopes was assessed by tetramer and intracellular cytokine staining (ICS). For tetramer stains, the percentages of live $CD3^+$ $CD8^+$ $tetramer^+$ lymphocytes are indicated while for ICS frequencies were calculated as responding $CD4^+$ or $CD8^+$ T-cells (i.e. $CD14^-$ $CD16^-$ $CD20^-$ $CD3^+$ lymphocytes of either subset producing any combination of IFN-γ, TNF-α, or CD107a together with CD69). Infected animals are indicated with an asterisk.

Mamu-A*02 tetramer

ID	treatment	dpi	**Gag GY9** (71-79)	**Vif WY8** (97-104)	**Nef YY9** (159-167)	**Env RY9 (296-304)**	**Env RY8 (788-795)**
rhBD70	PGT121-LALA	d219	0.003	0.005	0.000		
rhBD98*	DEN3	d219	**0.410**	**1.300**	0.008		
rhBE31*	PGT121-LALA	d219	**0.620**	**0.054**	**0.034**		
rhBB23*	DEN3	d219	0.075	0.000	0.002		
r08026	PGT121-LALA	d-1		0.012	0.000	0.008	0.048
r08026*	PGT121-LALA	d177		0.009	0.000	0.012	0.047
r08047	SIV-infected			**0.706**	**0.039**	**2.680**	**0.075**
rh2580	pre-infection	d-1	0.200	0.007	0.000	**0.015**	
rh2580	PGT121-LALA	d177	0.097	0.002	0.000	0.008	
r08047*	SIV infected		**0.294**	**0.706**	**0.039**	**2.680**	

Mamu-B*17 tetramer

ID	treatment	dpi	**Nef IW9** (165-173)	**Nef MW9** (195-203)	**Vif HW8** (66-73)
r03055*	PGT121	177	**0.180**	**0.005**	**0.007**
r09033*	PGT121	177	**0.830**	0.000	**0.015**
r04124*	PGT121	219	**1.400**	0.000	**0.190**
rhBB23*	DEN3	219	**0.700**	**0.002**	**0.011**
rhBD70	PGT121-LALA	219	0.003	**0.003**	0.003

Mamu-B*17 tetramer

ID	treatment	dpi	**Nef IW9** (165-173)	**Nef MW9** (195-203)	**Vif HW8** (66-73)
r08026	PGT121-LALA	-1	0.000	0.000	0.000
r08026*	PGT121-LALA	177	0.000	**0.003**	0.000
r08047	SIV-infected		0.000	**0.803**	**0.024**

Mamu-B*08 tetramer

ID	treatment	dpi	**Vif RL8** (173-181)	**Nef RL9a** (8-16)	**Vif RL9** (123-131)	**Nef RL10** (137-146)	**Rev KL9** (12-20)	**Rev RL8** (44-51)
r07036*	PGT121	219	**0.390**	0.003	**0.840**	**1.100**	0.003	0.015

Intracellular IFN-gamma and TNF-alpha

ID	treatment	dpi	no stimulus	**PMA/Ionomycin**	**Gag** (1-263)	**Vif** (whole ORF)	**Nef** (whole ORF)
r08026*, CD8+	PGT121-LALA	177	0.000	9.430	0.000	0.004	0.005
r08026*, CD4+	PGT121-LALA		0.000	5.130	0.002	0.000	0.000
r97104, CD8+	PGT121-LALA	177	0.000	12.1	0.02	0.01	0.005
r97104, CD4+	PGT121-LALA		0.000	5.88	0.000	0.001	0.002
rh2580, CD8+	PGT121	177	0.000	17.500	0.003	0.000	0.003
rh2580, CD4+	PGT121		0.000	9.330	0.004	0.002	0.005
rh2581, CD8+	PGT121	177	0.009	7.960	0.000	0.000	0.005
rh2581, CD4+	PGT121		0.000	8.690	0.000	0.000	0.004